

GOURC, J. P. and MONNET, J., IRGIM, Université de Grenoble, France
MOMMESSIN, M., LGCH, Université de Savoie, Chambéry, France

REINFORCED EMBANKMENTS ON WEAK SOIL: DIFFERENT THEORETICAL APPROACHES

VERSTÄRKTE DÄMME AUF WEICHEM UNTERGRUND: VERSCHIEDENE THEORETISCHE ANSÄTZE

RENFORCEMENT DES REMBLAIS SUR SOL MOU: DIFFERENTES APPROCHES THEORETIQUES

This paper has two aims :

To show that the finite element method takes in account the important differences between the behaviour of embankments reinforced with geotextiles and the non-reinforced ones; furthermore, this method allows quantification of the efficiency of a geotextile according to its stiffness.

To present a new method for the calculation of embankment limiting equilibrium, while taking into account the geotextile strains and the interface slipping.

An example of the application is presented, where the two methods are compared.

I. INTRODUCTION

The strengthening of embankments on weak soil using one or several geotextiles placed at the base of the embankment is a well known technique - BRAKEL et al(1). However, some progress may appear in the designing of these structures, in particular as regards the actual stresses applied in the geotextile and the required strains on the embankment and the subgrade required to apply these stresses. For this type of structure, which is likely to undergo great strain before failure, a theoretical approach to the study of settlement would greatly improve design.

At present, two methods of calculation can be distinguished:

The limiting equilibrium methods-JEWELL(3): distinguishes three modes of failure: rotational shear failure of the slope; slipping along the base of the geotextile embankment; overall punching of the weak soil subgrade. In order to take into account the composite character of the structure (soil and geotextile), partial safety factors relative to each component are used.

The finite element method: the main interest of these methods is that the behaviour of the soil, of the geotextile and of the soil-geotextile interface can be taken into account separately - ROWE (9); Mc GOWN et al (4).

The present paper has two aims:

To show, using a real case, that the finite element method shows clearly the very different behaviour of a non-reinforced embankment and an embankment reinforced by geotextile. This method can be used, in particular, to quantify the "efficiency" of a geotextile relative to its strain modulus J.

To suggest a new slope limiting equilibrium method, known as the "displacements method" - J.P. GOURC et al (2), A. RATEL (8), taking into account the fabric elongations and sliding at the soil interface, based on given kinematics. The usefulness of this method will be justified by comparative results obtained from the same real case using either the finite element method or the displacement method.

2. STUDY USING THE FINITE ELEMENT METHOD

2.1 Behaviour assumptions and modelling of materials and contacts:

The soil is presumed to behave as a standard elastoplastic material, following the DRUCKER-PRAGER or the TRESCA plasticity criterion. The elastoplastic analysis is performed using the initial stress method (7).

The geotextile transmits only tensile force along its plane. There is a linear relationship ($\alpha = J \epsilon$) between the tensile force per unit length of fabric and the relative elongation (plane strain).

Figure 1 shows the behaviour at the soil-geotextile interface, represented by isoparametric interface elements.

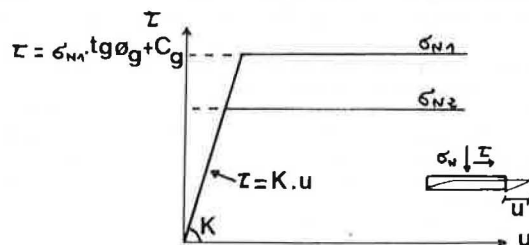


Figure 1 - Behaviour at the soil-fabric interface

2.2 GENERAL APPLICATION

Figure 12 shows the geometry of the structure. The characteristics of the materials are as follows:

Embankment: $E = 30,000 \text{ kPa}$; $\nu = 0.3$; $\phi_r = 35^\circ$; $\gamma_r = 18 \text{ kN/m}^3$; subgrade: E_u and C_u vary with depth (fig. 2); $\nu = 0.5$; $\gamma = 16.5 \text{ kN/m}^3$; active earth pressure coefficient, at rest $K_0 = 0.5$; embankment-fabric sheet interface: $\text{tg} \phi_g / \text{tg} \phi_r = 1$; $K = 2000 \text{ kPa/m}$; fabric sheet-compressible soil interface: $K = 1000 \text{ kPa/m}$; $C_g / C_u = 1$; the modulus of the fabric sheet J is taken as being

2B/1

variable from 0 kN/m ("non-reinforced embankment") to 1000 kN/m.

This study concerns plane strain.

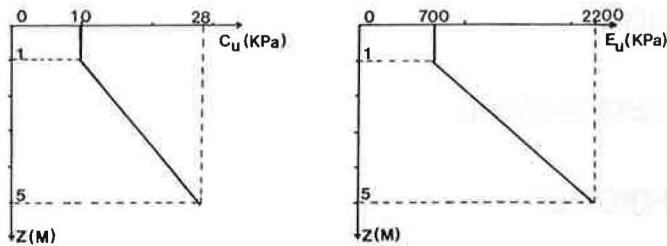


Figure 2 - Variation of E_u and C_u with depth

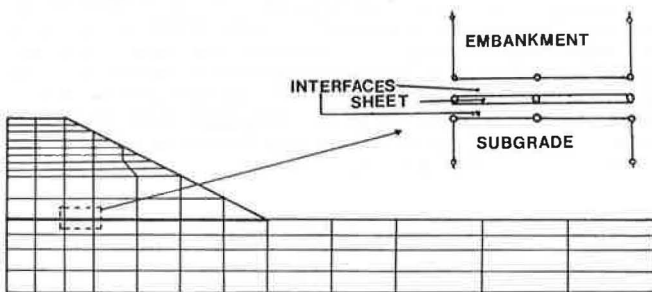


Figure 3 - Grid pattern used for model representation of the structure

Figure 4 shows, with a same embankment height H , a significant reduction of the plastic zones as the stiffness of the fabric sheet J increases. When the embankment is reinforced, the plastic zones develop, before failure, up to the axis of the structure. However, a non-plastified area remains at the base of the compressible layer. The behaviour of the structure is thus more comparable to that of a more or less rigid foundation (depending on the fabric sheet strain modulus) than to that of a non-reinforced embankment undergoing a circular failure.

As regards plasticity, a structure is considered as failed when plastic zones appear that are not contained within the elastic zones, as illustrated by figure 5a for a non-reinforced structure or in the case of a failure of the fabric sheet; and by diagram 5b with a non-failed geotextile, which is considered as an elastic medium. In order to reach this failure, C_u was made to vary progressively with H varying from 4 meters to 6 meters (fig.6). It is noted that, for a given stiffness of the fabric sheet, the coefficient $C_n(z=0)/(\gamma \cdot H)$ is practically constant at the moment of failure. Figure 7 shows a rapid decrease of this coefficient for low values of J , showing a significant gain in safety.

The stiffness of the fabric sheet has little influence on the settlement along the axis at the embankment head (point A in figure 12). Significant deviations appear only in the vicinity of the failure. The differential settlement (between A and C) decreases as the stiffness of the fabric sheet increases: it changes from 38% for $J = 0$ KN/m, to 30% for $J = 200$ KN/m and to 18% for $J = 1000$ KN/m. ($H = 4.5$ m) Maximum stress in the fabric sheet occurs above to the plastified zones. At equal height, the stress increases with the stiffness of the fabric sheet (figure 8). Inversely, the maximum elongation of the fabric sheet decreases with stiffness (fig.9) The selection of a geotextile sheet is thus confronted with two contradictory criteria: a non-rigid fabric sheet which would limit tensile forces, or a rigid fabric sheet which would limit strain.

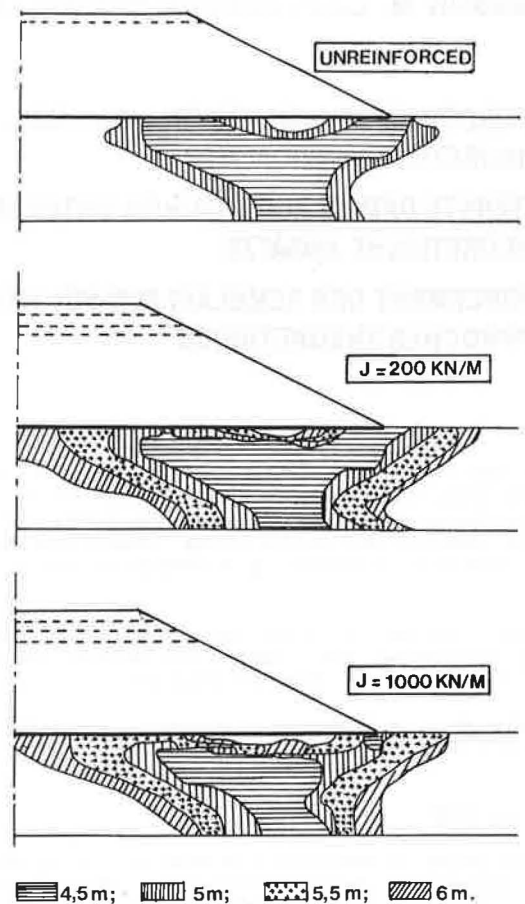


Figure 4 - Development of the plastic zones in the subgrade relative to the stiffness of the fabric sheet and the embankment height.

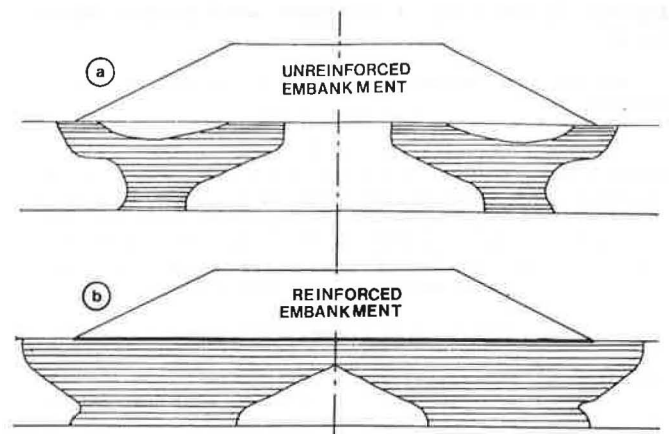


Figure 5 - Principle of plastic zones in the subgrade on failure.

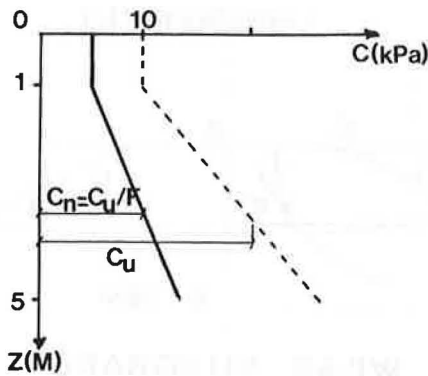


Figure 6 - Development of the subgrade cohesion up to failure.

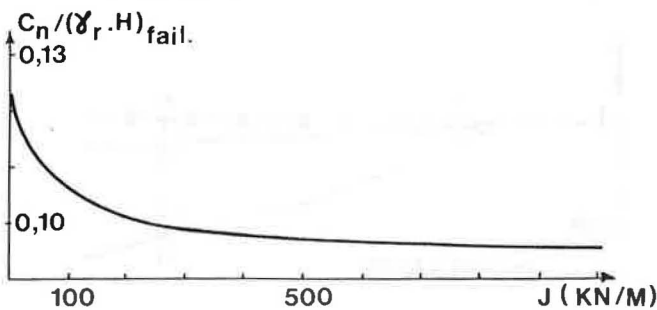


Figure 7 - Variation of $C_n(z=0)/(\gamma_r \cdot H)$ at failure, relative to fabric stiffness.

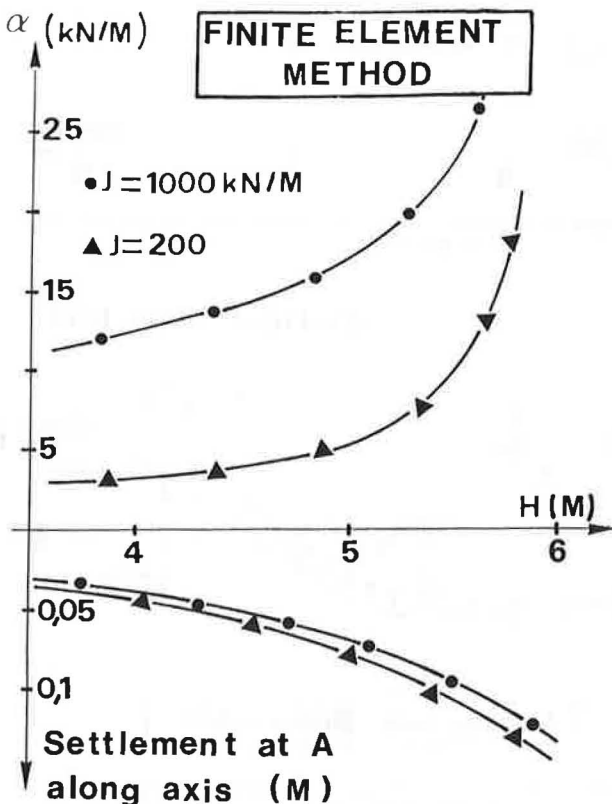


Figure 8 - Maximum stress in the geotextile and settlement along the axis relative to embankment height.

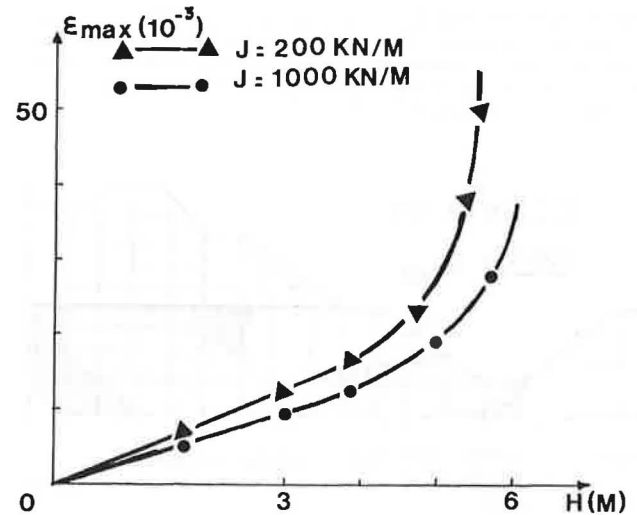


Figure 9 - Maximum elongation of the geotextile relative to embankment height.

2.3 The study of ALMERE embankment :

The detailed report on the behaviour of a reinforced and a non-reinforced embankment constructed up to failure, appeared in (1). This structure will be the subject of the present study. The mechanical characteristics retained for the embankment are $E = 30000 \text{ kPa}$; $\nu = 0.3$; $\phi = 45^\circ$; $\gamma_r = 18 \text{ kN/m}^3$. For 3m thick compressible soil: $E = 7000 \text{ kPa}$; $\nu = 0.5$; $C_u = 8 \text{ kPa}$; $\gamma = 13 \text{ kN/m}^3$; $K_o = 1$. For the reinforced section: geotextile $J = 2000 \text{ kN/m}$; embankment-geotextile interface: $K = 2,000 \text{ kPa/m}$; $\phi_g = 45^\circ$; subgrade geotextile interface: $K = 1,000 \text{ kPa/m}$, $C_g = 8 \text{ kPa}$.

Non-reinforced section:

The development of the plastic zones in the subgrade soil is shown in figure 10, which also shows the critical slip circle obtained using a classic slope stability method for the experimental failure height (a safety factor $F = 0.91$ is thus obtained). A rapid evolution of the plastic zone is noted for heights greater than 1.5 m.

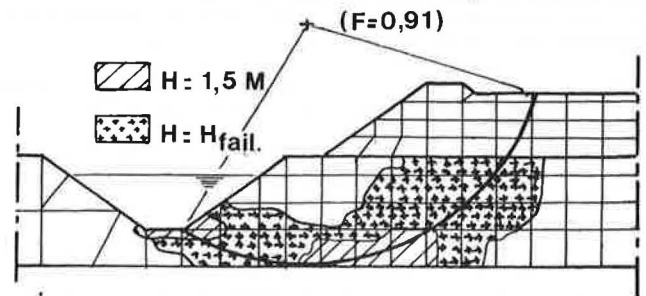


Figure 10 - ALMERE embankment, non-reinforced section ; development of plastic zones in the sub-grade soil and critical slip circle.

Reinforced section:

Figure 11 shows the development of the plastic zones. For the experimental failure height, there is no convergence with the elastoplastic analysis (the theoretical failure height is exceeded); the plastic zones easily reach the axis of the structure. The maximum stress in the fabric sheet is 30 kN/m for a height 2.5 m and is

greater than 50 kN/m (no convergence) for the experimental failure height. The maximum experimental tensile force 95 kN/m. An strained geometry calculation rather than an initial geometry calculation would no doubt lead to comparable tensile forces.

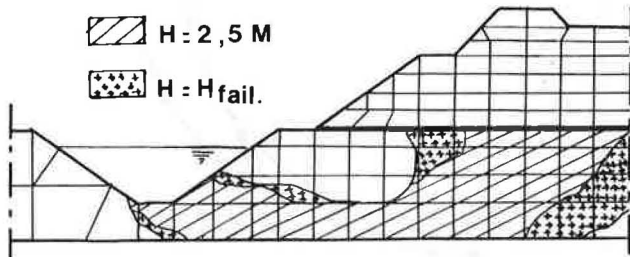


Figure 11 - ALMERE embankment, reinforced section. Development of plastic zones in the subgrade soil.

3. DISPLACEMENT METHOD:

As a reference (2), we suggested a new design method, known as the "displacement method". This method will be applied to the example treated above (figure 12). The principle is as follows: Beyond the ultimate height of the non-reinforced embankment ($H = 4$ m), the presence of a geotextile does not prevent rotational slipping of the slope, but does limit rotation. A new limiting equilibrium is obtained, on the one hand due to displacement of the centre of gravity of the zone in movement ("ad" in figure 13), on the other hand due to the stressing of the geotextile ("dc" in figure 13).

Note however, that even for a reinforced embankment, the height of the embankment will be limited by the overall punching stability, as was shown in the previous chapter. By using the hypothesis which supposes that the geotextile functions as an embedded membrane (figure 14), the force α_j and the angle of inclination β_j of the geotextile can be determined at the point of intersection with the slip surface, for each rotational increment $d\theta$.

The method of stability by limiting equilibrium is known as the disturbance method. The rotation required for equilibrium is such that:

$$- M_1 (\alpha_j) + M_2 \text{ restoring (shearing of the soil)} + M_3 \text{ disturbing (weight of soil in rotation)} = 0.$$

In the present application, moments M_1 and M_3 vary with $\Delta\theta$, but M_2 is taken as constant (with the residual soil shearing characteristics).

Note, in figure 13, that for a geotextile with a lower strain modulus $J = 200$ kN/m, the gain on the safety factor in conjunction with the rotation of the slope is relatively higher than that obtained from the force α_j on the geotextile, due to the relatively high equilibrium rotation.

In effect, note in figure 15 that as high is the geotextile modulus, as low is the equilibrium rotation.

The present method offers several advantages over the standard limiting equilibrium methods used:

No orientation is required for the force α_j , which is determined from the equilibrium; secondly, the strain modulus J of the geotextile is taken into account.

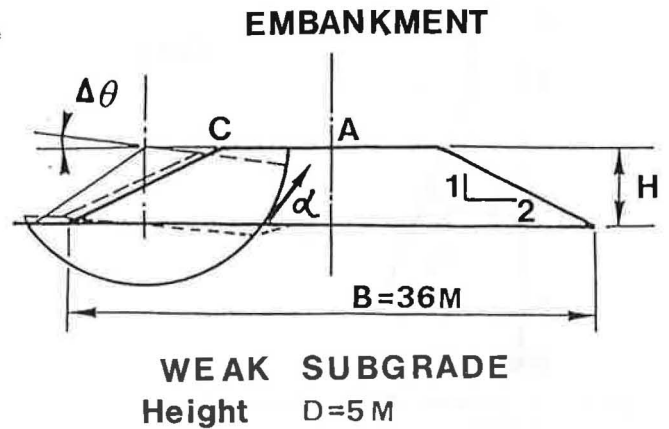


Figure 12 - Example of a reinforced embankment

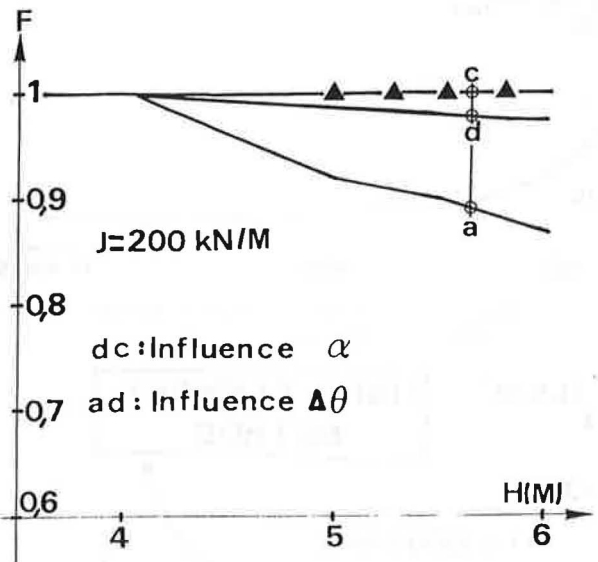


Figure 13 - Evolution of the reinforced embankment safety with height.

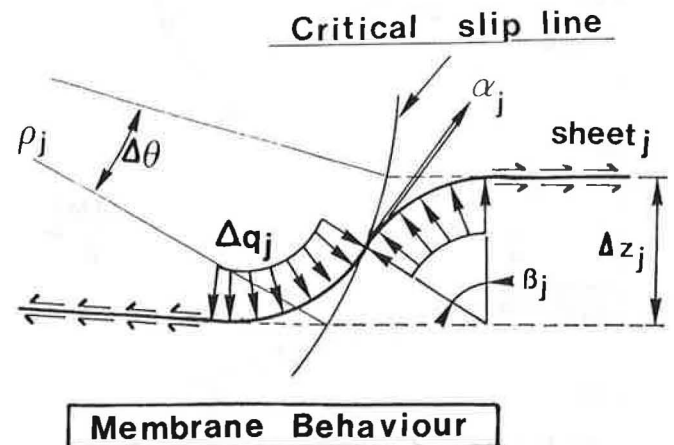


Figure 14 - Behaviour of the (membrane effect) geotextile in the vicinity of the slip surface.

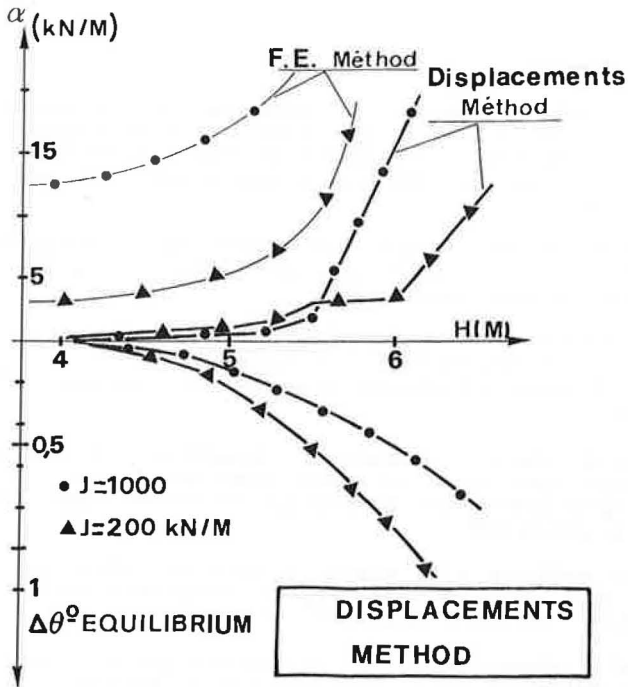


Figure 15 - Comparison between the finite element method and the displacement method.

However, one point remains to be made clear, which will be dealt with in the following chapter: the membrane curvature of the fabric depends on the stiffness K_s of the soil (in the present example, we have taken $K_s = 1000 \text{ kN/m}^3$) with $\Delta q_j = K_s/4 \cdot \Delta z_j$. The study presently beginning at the University of Grenoble should clarify this point.

The comparison of forces α_j as a function of the modulus J and the height H of the embankment shows a high compatibility, relative to the uncertainty of the stiffness factor K_s .

4. EXPERIMENTAL AND THEORETICAL APPROACH TO MEMBRANE BEHAVIOUR:

4.1 Experimental apparatus:

In order to study the phenomenon of tensile stressing of the geotextile at the failure surface, we performed a direct shear test in a large-scale box 800 mm long and 250 mm high containing sand and geotextile. A compressive stress was applied and the developed tensile force inside the reinforcing structure was measured.

4.2 Theoretical model representation:

The box is represented in figure 16. The geotextile fabric simulated is 4 mm thick non-woven needled polyester with a bulk specific gravity 1.2 kN/m^3 . It is modelled by a double layer of quadrilateral elements with 8 nodes of Young's modulus 12 KN/m^2 and a Poisson's ratio of 0.3. The soil is sand with $\gamma = 15.8 \text{ KN/m}^3$.

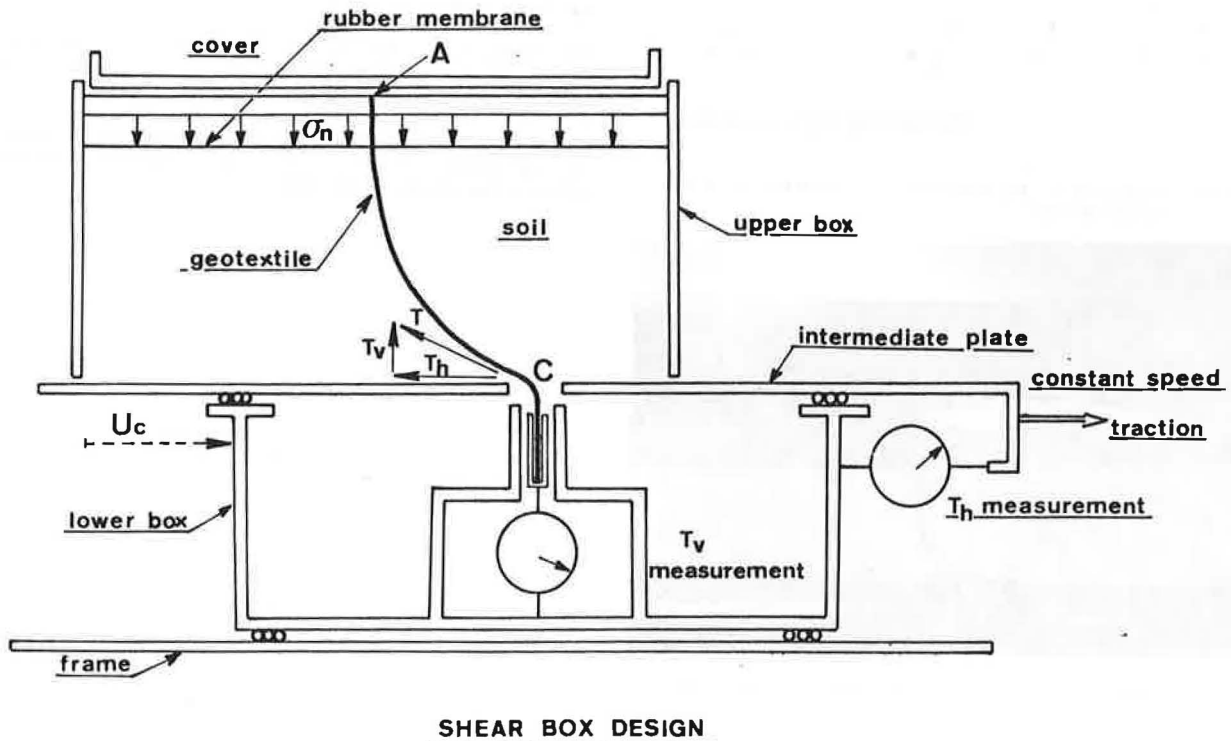


Figure 16 - Diagram showing the membrane effect box

Its behaviour is represented by the law with plane strain work hardening (Monnet) (6). The main interest of this model is to produce a precise representation of soil shearing with dilatancy, using only 4 parameters ($E = 31,600 \text{ KPa}$, $\nu = 0.3$; $\phi_u = 28.4^\circ$; $\phi = 39.6^\circ$). The plasticity effect taken into account is non-standard plasticity.

4.3 Theoretical results

For this calculation, a pressure of 30 KPa was applied to the soil surface and the lower part was displaced in order to cause shearing of the geotextile. The strain of the fabric is obtained (figure 18). Note also, as great are the displacements, as curved is the geotextile.

These first results, although partial, show that the theoretical curves provide a correct representation of the real phenomena. They also show the importance of taking into account large strains.

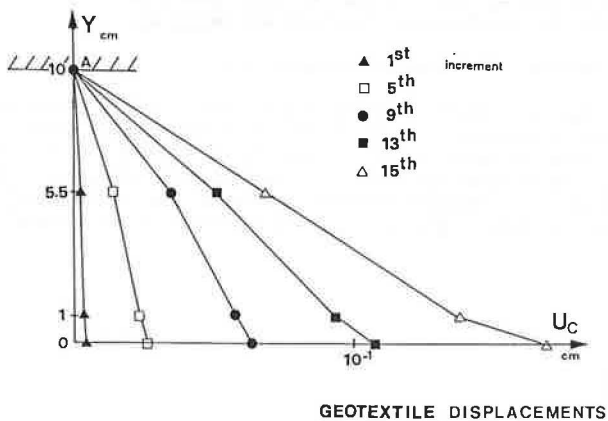


Figure 18 - Geotextile deformation (finite element calculation)

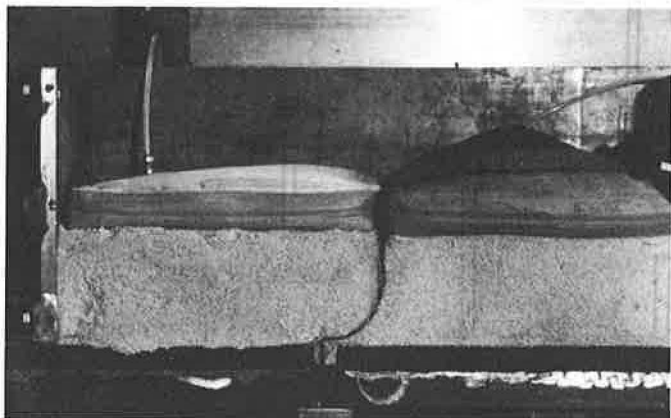


Figure 17 - Membrane effect test apparatus (piston removed).

ACKNOWLEDGMENTS

The authors thank J. BELISLE for his support to translation.

REFERENCES

- (1) BRAKEL J. - COPRENS M. - MAAGDENBERG A.C. - RISSEEUW P.: Stability of slopes constructed with polyester reinforcing fabric, test section at Almere, Holland 79 - 2nd International Conference of geotextiles - Las Vegas USA 1982.
- (2) J.P. GOURC - A. RATEL - Ph. DELMAS: Calculs des murs en sol renforcé - 3rd International Conference of geotextiles - Vienna - Austria 1986.
- (3) JEWELL R.A.: A limit equilibrium design method for reinforced embankments on soft foundations - 2nd International Conference of geotextiles - Las Vegas USA 1982.
- (4) Mc GOWN A. - ANDRAWES K. - MASHOUR M. - MYLES B.: Strain behaviour of soil-fabric model embankments - 10e congrès international de Mécanique des Sols et Fondations - Stockholm 1981.
- (5) MOMMESSIN M.: Remblai renforcé par géotextiles, étude par éléments finis - Rapport interne de recherche - IRIGM - Université de Grenoble - France - 1984.
- (6) J. MONNET: Calcul au cisaillement du sable sollicité en déformation plane" Revue Française de Géotechnique n° 21 - p. 41 - 45 - 1982.
- (7) G.C. NAYAK, O.C. ZIENKIEWICZ: Elasto-plastic stress analysis. A generalisation for various constitutive relations including strains softening international Journal for numerical methods in Engineering, vol. 5 - pp. 113 - 135 - 1975.
- (8) RATEL A.: Massif en sol renforcé - Principe de calcul de la méthode en déformations - mémoire DEA - IRIGM - Université de Grenoble - France 1984.
- (9) ROWE R.K.: The analysis of an embankment constructed on a geotextile - 2nd International Conference of geotextiles - Las Vegas - USA 1982.